Analysis of ngVLA Design #6 With Ideal and Actual Feed

Lynn Baker

January, 2017

Document #: 020.25.01.00.00-0001-REP ngVLA Optical Reference Design

Introduction

This document presents a first design targeting a high efficiency design for the ngVLA. A new aperture illumination function and its corresponding mapping function underlies this shaped design. The ngVLA specifications allow for higher than typical near in sidelobes which allows for a nearly uniform, high efficiency aperture illumination. However, a high efficiency design still must have very low spillover so that noise temperature is minimized. The design presented here achieves both of those goals along with very low intrinsic cross polarization and excellent beam symmetry.

High Efficiency Mapping Function

A new mapping function which provides very high illumination efficiency has been developed and implemented in the dual reflector shaping software. This function gives a uniform aperture illumination over almost all of the aperture with a sharp roll off near the edge. The function is a scaled and translated version of a hyperbolic tangent function. The equation for this function is displayed in Figure 1 where it is plotted for the parameters used in this design. The parameter t sets the steepness of the roll off and x0 is chosen indirectly to give the desired edge taper at scaled radius = 1. Figure 1 is for t=10 and x0 is chosen to give an edge taper of .1, -10 db. The calculated efficiency of this illumination is .95. It is to be expected that an illumination this uniform will result in higher than typical near in sidelobes.

This function has several useful features besides its general shape of being flat over most of the aperture. It is continuous with continuous derivatives and is composed of a single function over the whole span. It is integrable in closed form on the unit disk (by Mathematica) which makes manipulations to obtain the mapping function easier. It does not go negative for scale radii above 1 which allows shaping the reflectors with extension points beyond the nominal physical edges.

Figure 1

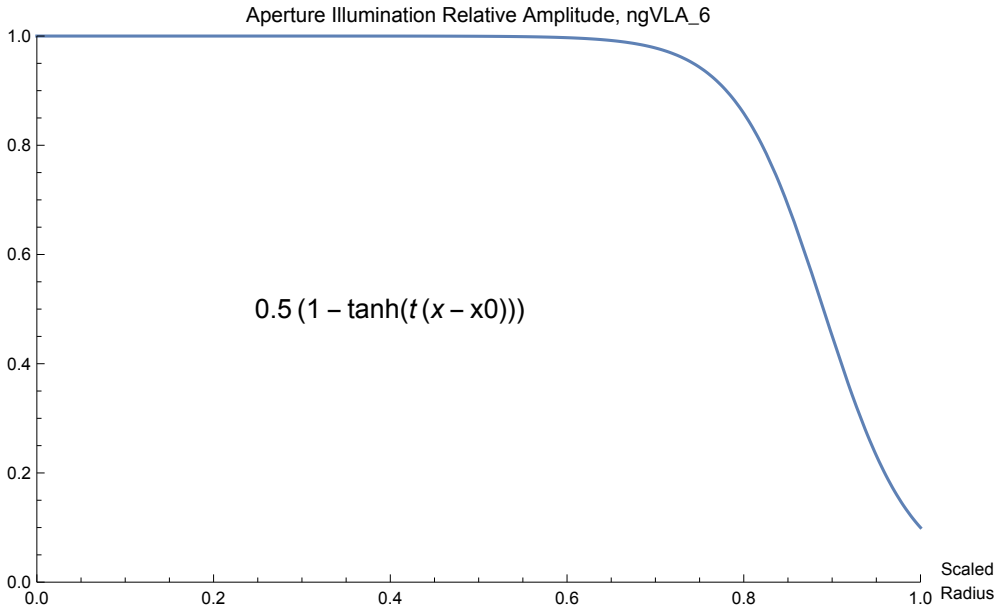

The desired mapping from the feed to the aperture is provided by the transformation given by the shaped optics. The feed pattern function here is taken as a cosine raised to a noninteger power. The power is chosen to give the desired edge taper on the rim of the subreflector. This function also integrates in closed form in spherical coordinates. In this design the edge angle is 55° and the chosen edge taper is -16 db. Transforming this deeply tapered feed pattern to the aperture illumination shown in Figure 1 requires significant redistribution of power which is described by the the mapping function shown in Figure 2. This curve is obtained by equating the integral power inside a given elevation angle at the feed to the same integral power inside the corresponding radius in the aperture. The plot is scaled by the maximum elevation angle and aperture radius so the curve goes from the point 0,0 which is the central ray out to the point 1,1 which is a ray on the edges of the subreflector and primary. The plot extends beyond the point 1,1 so the the reflector shapes can have extension points beyond the physical edges. The dashed straight line passes through the points 0,0 to 1,1 and is close to what a conic section design produces.

Figure 2

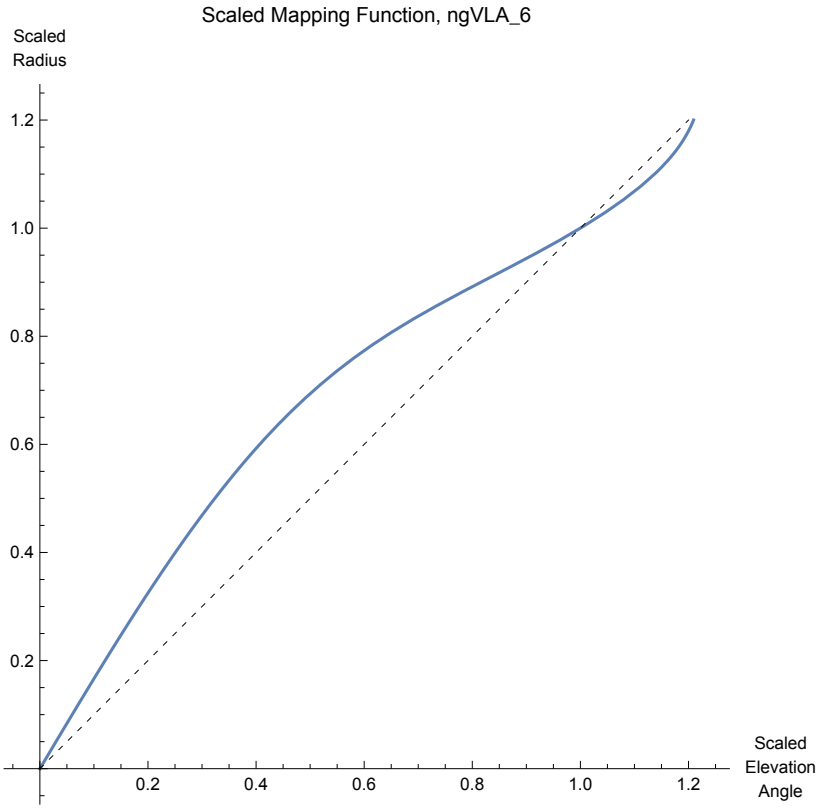

The effect of the mapping function can be described as follows. Near the center of the reflectors the slope of the map is greater than the straight line which gives a larger increment in radius for a given increment in elevation. This results in the intense central peak of the feed pattern being spread out over a larger area in the aperture plane, reducing its intensity. Near the middle of the map the slope is the same as the line and the spreading is moderated. In this area the feed pattern is lower and less spreading gives an aperture intensity which is the same as near the center. Beyond the middle the slope of the map is less than the line and this corresponds to the feed intensity being squeezed to raise the intensity in the aperture. The feed pattern is even smaller in this region and the squeezing keeps the aperture intensity uniform. At the very end the slope starts to increase again which along with the very low feed intensity provides the sharp roll off in intensity at the very edge of the aperture. The resultant intensity in the aperture is quite sensitive to small changes in the mapping function because of this derivative behavior. This requires a lot of attention to the calculation and software implementation of any mapping function.

Optical Design and Reflector Geometry

Figure 3 shows the cross section of the optical design implementing the mapping function. The geometric parameters are the ngVLA specifications: an 18 meter diameter aperture, a 3.5 meter diameter subreflector and a 55° half opening angle. This design has the subreflector spaced a longer distance from the lower, left edge of the primary. This has be beneficial effect of reducing the tilt angle of the primary and making it somewhat smaller at the expense of a longer feed arm. This choice of this geometry was made in collaboration with the structural design team. The tilt angle of the central ray from the focus is optimized to give low cross polarization, analogous to the Mizugutch condition in conic sections.

The numbers above the secondary and below the primary are the rim to rim distance, the area of the surface and the area of the surface as a fraction of the aperture area.

The behavior described in the mapping section can be seen in the cross section of the optics shown in Figure 3. The rays emanating from the focus are equally spaced in elevation angle. The spacing of the rays in the aperture is larger near the center and get progressively closer together moving outward. The last radial increment at the edge is slightly bigger which contributes to the deep roll off in intensity there.

For reference when discussing the physical optics analysis, note the distance from the focus to the surface of the secondary varies by roughly a 2:1 ratio across the span of elevation angles. At lower frequencies this places the left part of the secondary in the near field of the feed. Another effect is that the area on the secondary inside a quadrilateral formed by four adjacent rays varies by the same 2:1 ratio. These effects combine to blur the illumination of the secondary towards the primary in the vicinity of the ray going to the far right edge of the primary. This gives a progressively larger spillover over the right edge of the primary at lower frequencies.

Figure 3

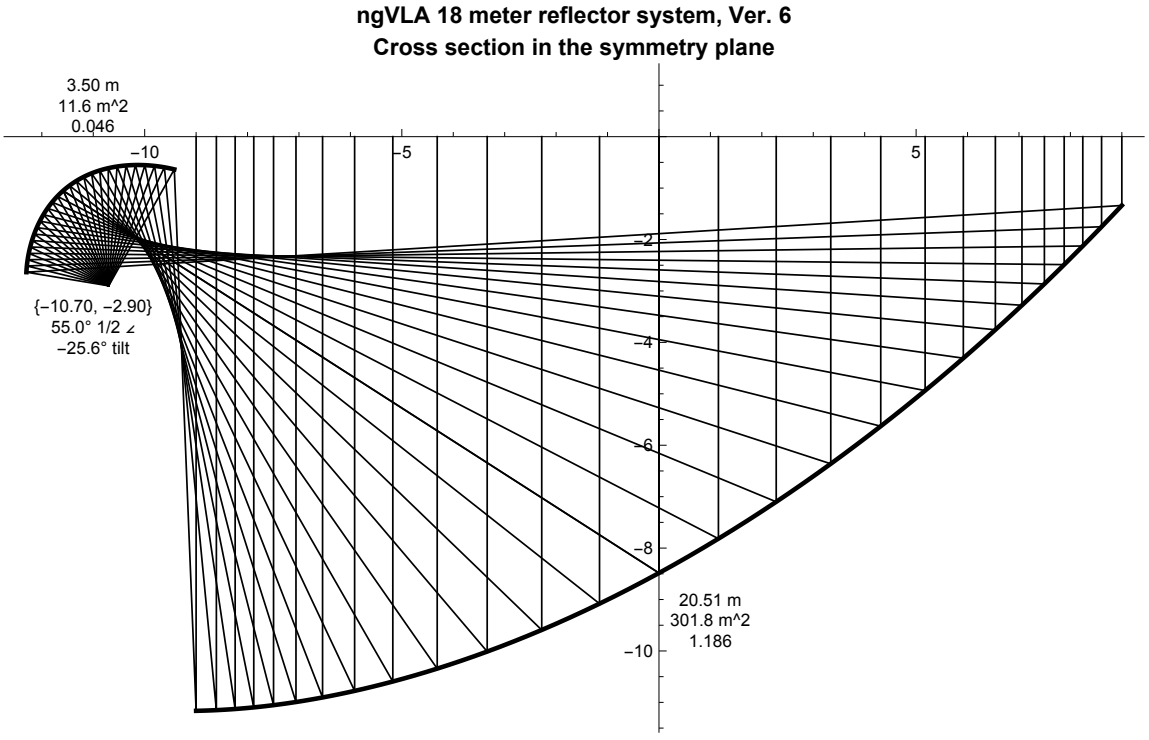

Physical Optics Analysis with an Ideal Feed

The geometry shown in Figure 3 was imported into GRASP for analysis. The first analysis is done with an ideal gaussian feed pattern having a -16 db. edge taper at 55°. This is slightly different than the cosine function used to develop the mapping function but is the best available choice in GRASP. This first analysis was performed at 5 GHz. which is good compromise between fast runs and avoiding most low frequency diffraction effects. Analyzing the optics with a perfect feed establishes a baseline performance so the effects of a real feed can be seen separate from the optics performance.

The copolar aperture illumination on the plane at z=0 is shown in Figure 4. The illumination is nearly uniform across the aperture with a steep roll off at the edge. This confirms that the design mapping function was successfully achieved. Although obscured by the wide logarithmic scale, there is some diffraction ripple across the aperture plane which is expected since the z=0 plane is some distance

from the primary reflector. The left side of the plot shows the interference effects of the feed spillover interacting with the aperture illumination. This does not effect the main beam performance since the spillover and aperture project to different angles in the far field.

Figure 4

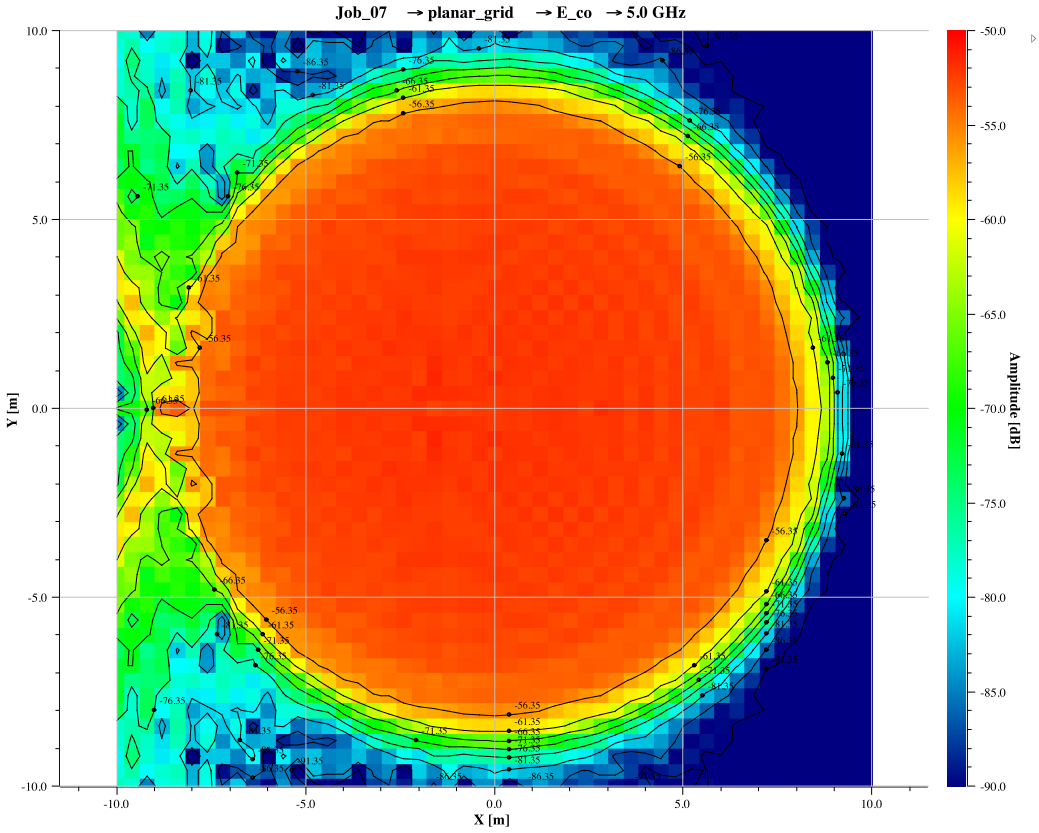

Figure 5 shows the close in far field pattern in three azimuth cuts at 0°, 45°, 90°. The vertical scale is gain over isotropic in db. The peak gain is 59.0 db. which corresponds to an overall efficiency of .89. The illumination efficiency is .95 and the feed spillover past the secondary is a factor of .98. Other small factors combine to give the final overall efficiency. The first sidelobe level is -19 db. below peak. The second sidelobe level about -27 db. These values are higher than typical designs with conics and result from the nearly uniform aperture illumination. The maximum cross polar level is about -45 db. below the main beam peak. The cross polarization is everywhere zero in the symmetry plane and peaks in the plane perpendicular to the symmetry plane. The intrinsic cross polarization of the optics is very small, smaller than the cross polarization introduced by any realistic feed. The rotational symmetry of the main beam is essentially perfect.

Figure 5

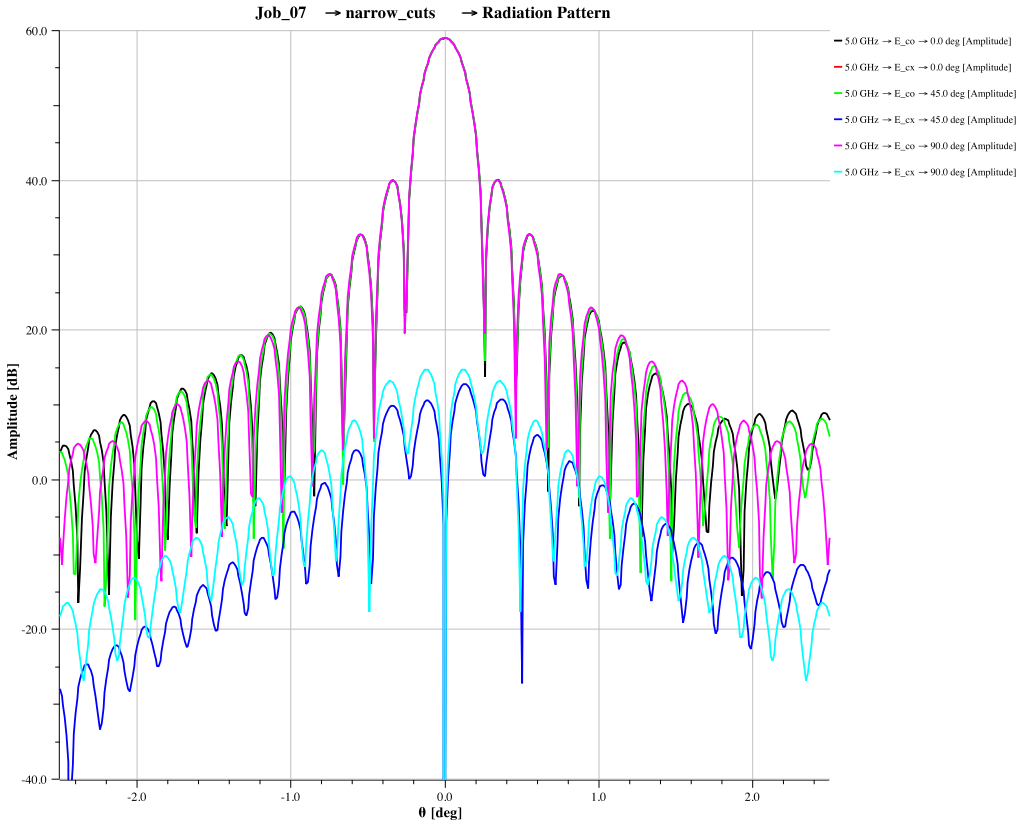

To better understand the wide angle pattern and especially the tipping curve it is useful to visualize the entire far field sphere to see the general features. Figures 6,7 show the far field sphere in two halves, the north and south hemispheres. Each hemisphere is projected and plotted on a unit disk which distorts the view slightly but still gives a good sense of the features. The color bar gives the scaling in dbi.

There are two main features outside of the main beam at the north pole. In the north hemisphere the feed spillover past the secondary is very clear. The feed tilt angle is about -25° with an opening angle of +-55°. In the symmetry plane the spillover is just past the geometric edges at -80° and 30°. Perpendicular to the symmetry plane, the spillover is just past +-55°.

On the right of the north hemisphere there is a small part of the secondary spillover past the primary. This area corresponds to the ray which goes from the left edge of the secondary to the right edge of the primary and is slightly above the horizon. Looking at the arc of the secondary spillover above the horizon shows it is slightly more intense than the rest of the secondary spillover seen the the south hemisphere. As discussed above, this is due to that part of the secondary being closer to the focus. The effect is very minor at 5 GHz. and will get smaller at higher frequencies and larger at lower frequencies.

Figure 6

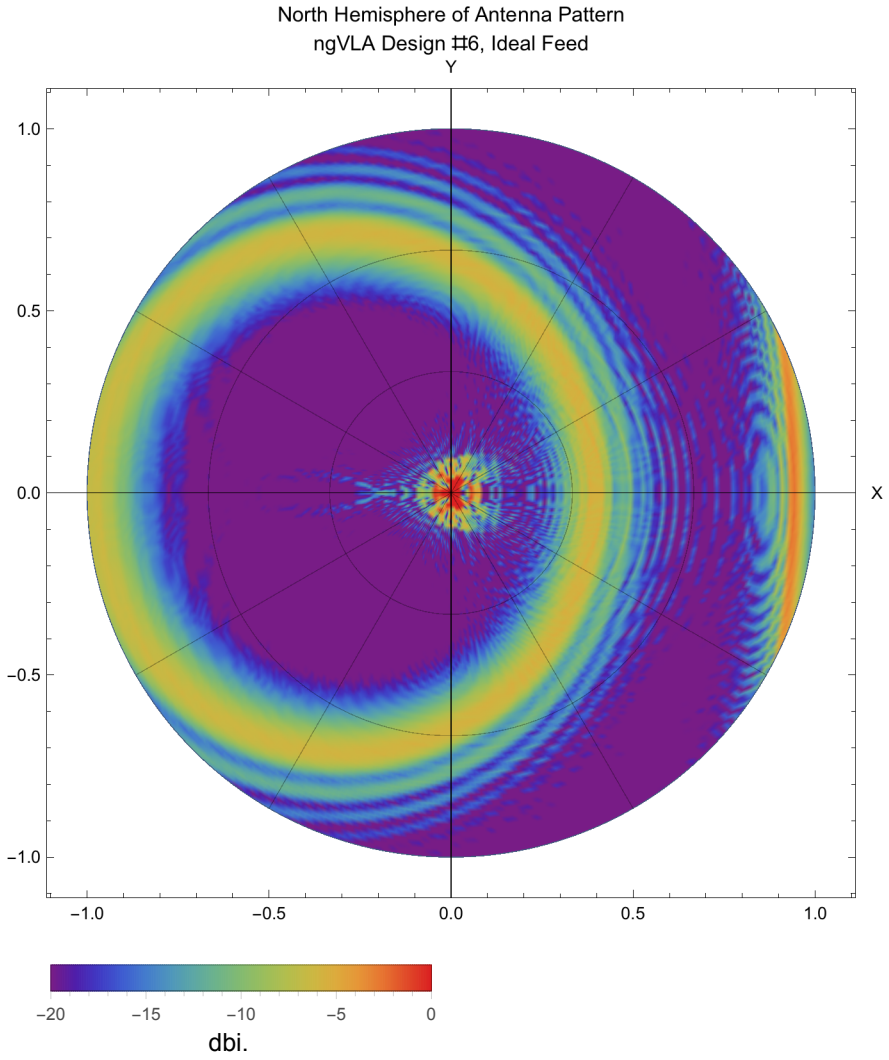
North Hemisphere of Antenna Pattern
ngVLA Design #6, Ideal Feed
Y
X
1.0
0.5
0.0
−0.5
−1.0
−1.0
−0.5
0.0
0.5
1.0
−20
−15
−10
−5
0
dbi.

Figure 7

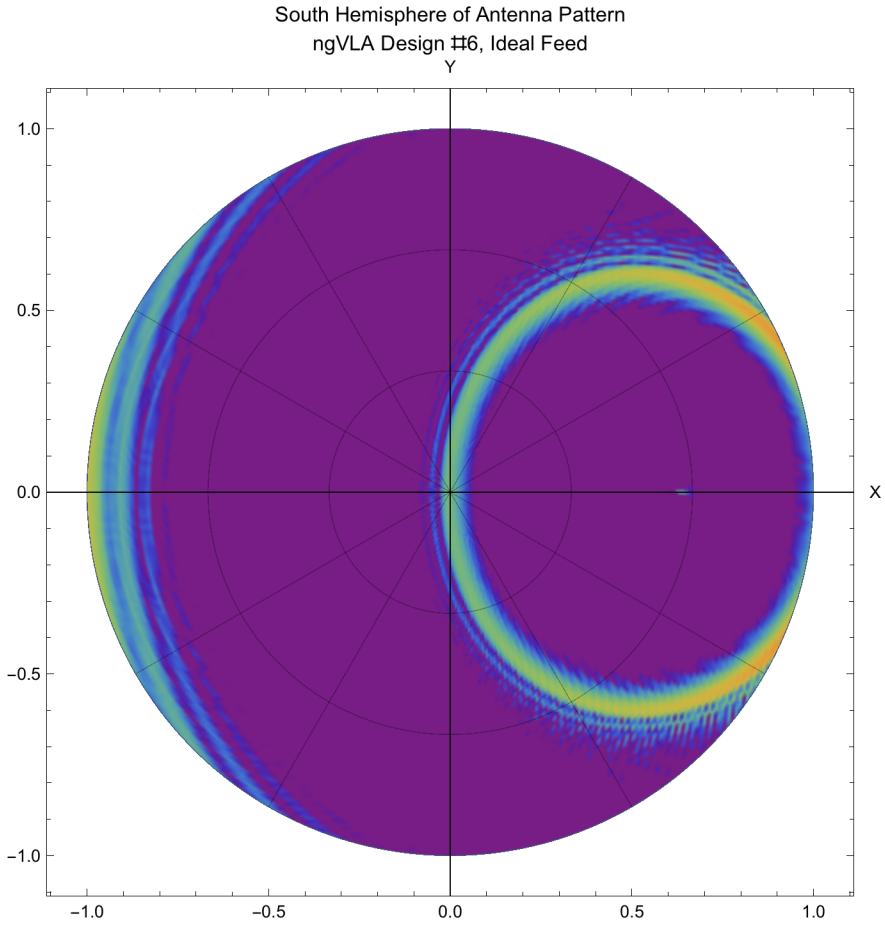

Figure 8 shows the far field pattern over the entire range of elevation angles and the same three azimuth cuts. The main feature here are the very low wide angle sidelobes. The peaks of the wide pattern are at least -6 db. below isotropic except the small peak at 85° which is the spillover past the primary discussed above. The other peaks correspond to various parts of the feed spillover as shown above.

Figure 8

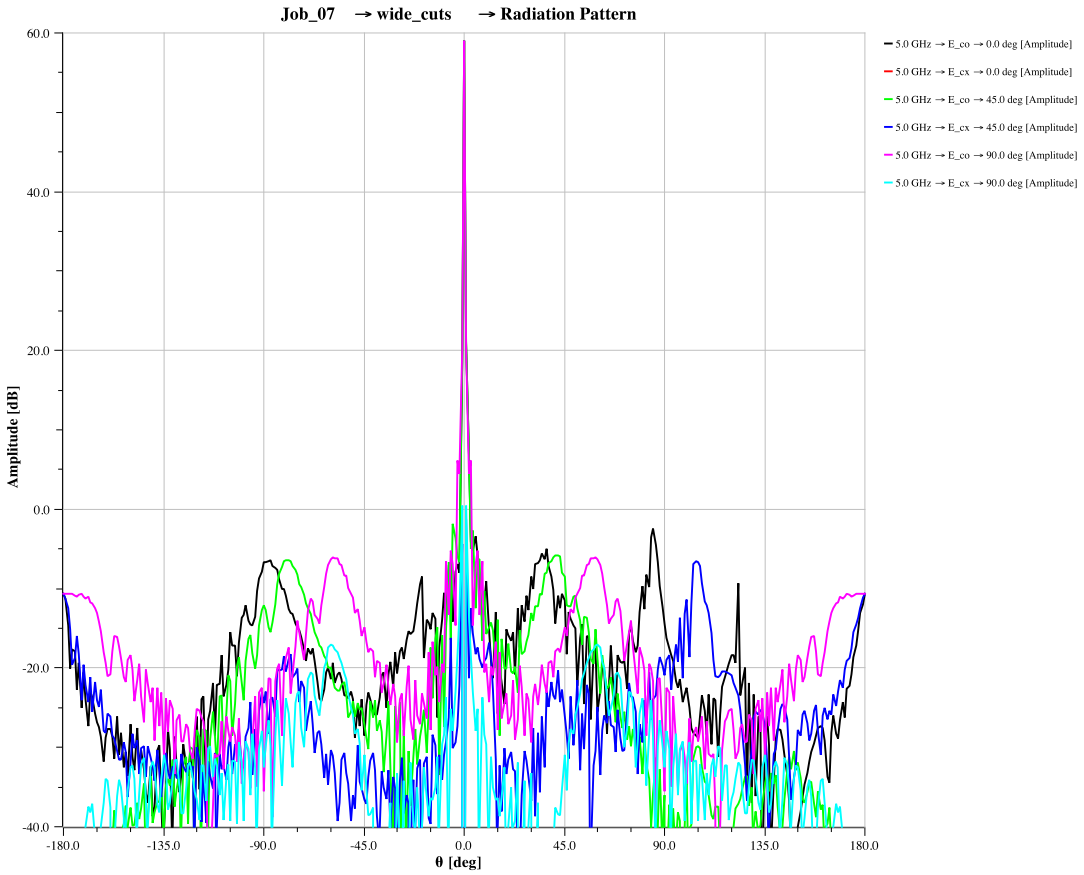

There is one effect which might slightly disturb far field main beam. The edge diffraction past the rim of the secondary fans out in a range of angles some of which are essentially parallel to the main beam. This small contribution to the main beam has a different path length and goes in and out of phase with varying frequency. This produces a small gain ripple versus frequency on boresight. This effect was first documented by the South African MeerKat/SKA team. In this case it is mitigated by the very deep edge taper on the secondary. A future calculation could quantify its effect here.

Tipping Curve with an Ideal Feed

A key parameter of the antenna design is the contribution to system noise temperature from spillover outside of the main beam area at all pointing angles. To calculate this a model of the noise environment surrounding the the antenna is required. Figure 9 shows the SKA standard noise model at 5 GHz. Comparison with site specific data at the VLA site shows this model to be slightly pessimistic in the upper hemisphere. The contribution of the receiver is not included in these plots.

To compute the tipping curve the noise model is multiplied by the antenna pattern at various tilt angles and integrated over the sphere. To simplify the calculation the simple noise model is tilted instead of the complicated antenna pattern but the result is the same.

Figure 9

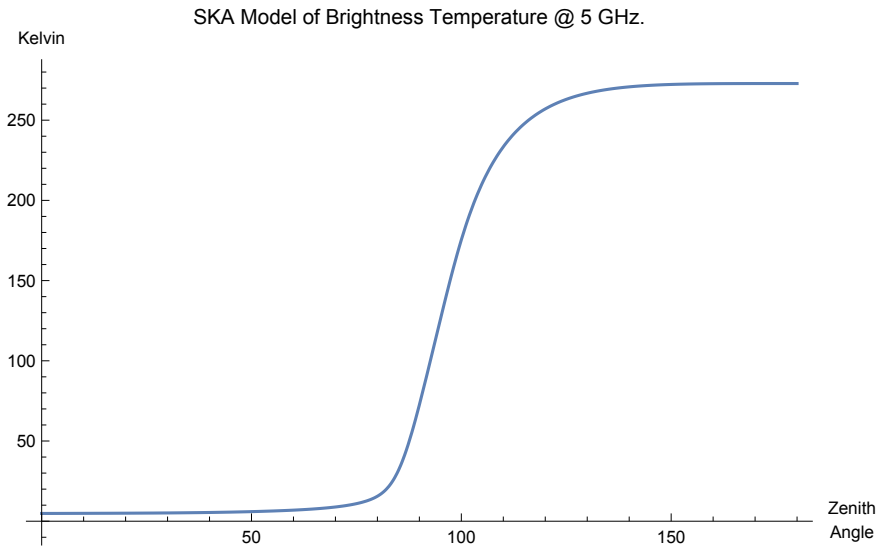

The result of the calculation is shown in Figure 10 for both feed arm up and feed arm down pointing. The noise model is also shown so that the effect of spillover can be directly seen. If the antenna pattern was a delta function then the tipping curve would be the same same as the noise model. Any difference is due the small wide angle spillover illuminating various parts of the noise model.

There is only a small difference between feed up and feed down pointing. Feed arm down pointing steadily rotates the feed spillover on to the warm ground while the spillover past the primary rotates up on to the cold sky. In this case the the feed spillover is a bit larger so the net effect is a slightly larger noise increase. The converse happens for feed up pointing. The feed spillover stays on the sky until at larger zenith angles where the part at +30° crosses the horizon. The smaller spillover past the primary rotates completely on the ground and stays there.

The MeerKAT and SKA antenna designs from the South African design team have an extension on the lower edge of the subreflector which redirects part of the feed spillover to over the far edge of the primary. For feed arm down pointing this mitigates the effect of the feed spillover striking the ground and gives a better result. Such an extension could be investigated as an addition to this design. Another possible way to improve the tipping curve would be increasing the edge taper on the secondary to a level below -16 db., capturing more of the feed energy in the optics.

Reiterating a point discussed before, the slightly larger spillover due to diffraction effects on the secondary will get larger as the frequency goes lower. In the SKA case where the operating frequency goes well below 1 GHz. it gets very large and dominates the tipping behavior. Conversely, at frequencies higher than the 5 GHz. here, it will get even smaller.

Figure 10

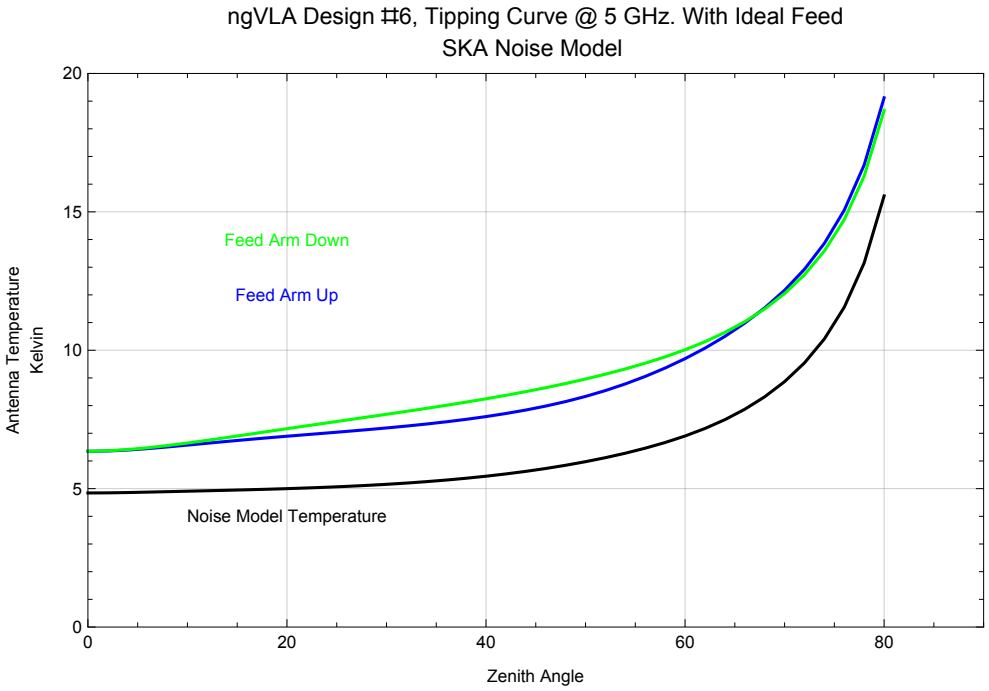

For comparison to other designs and reports, Figure 11 plots the difference between the noise model and tipping curves in Figure 10. Leaving the details aside, the spillover noise contribution is very small overall. At the higher frequency bands of the ngVLA the sky and receiver temperatures will dominate over this small contribution.

Figure 11

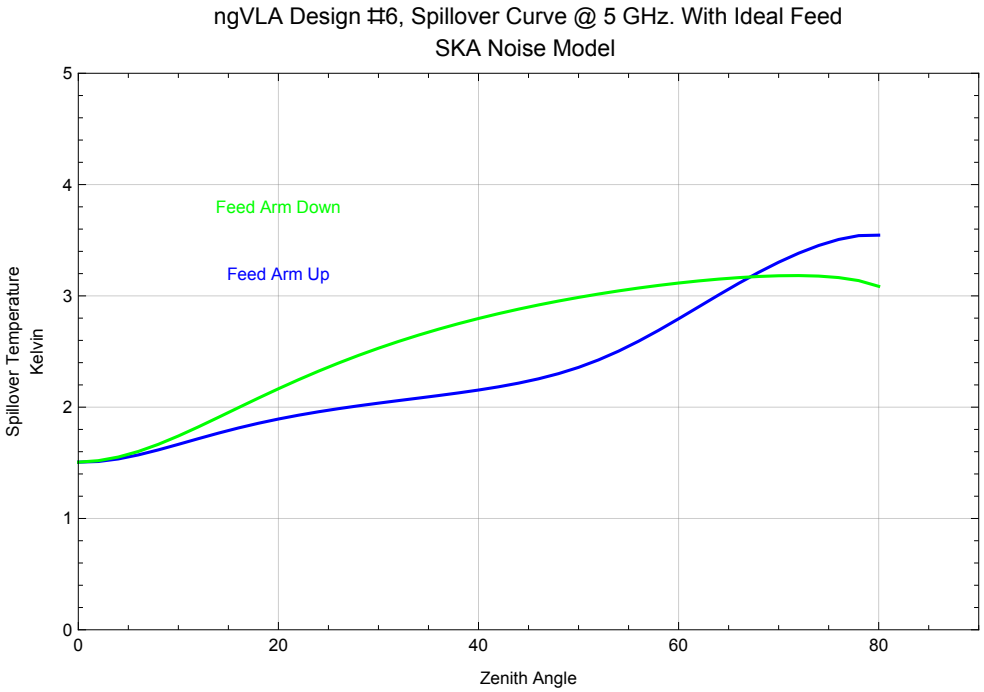

Physical Optics Analysis with an Actual Feed

The optics are next analyzed with the corrugated horn feed shown in Figure 12 with the pattern plot in Figure 13. This axial ring design was developed for the DVA1 project at L-band. It has excellent performance over an octave bandwidth and is compact, an important trait at L-band. The original L-band design was scaled to the frequency range of 4 to 8 Ghz. which places the 5 GHz. analysis frequency in the lower part of the frequency coverage.

The performance with this feed is very close to the performance with a perfect feed. The commentary in the previous sections applies with small changes so only the differences in the two cases will be discussed.

Figure 12

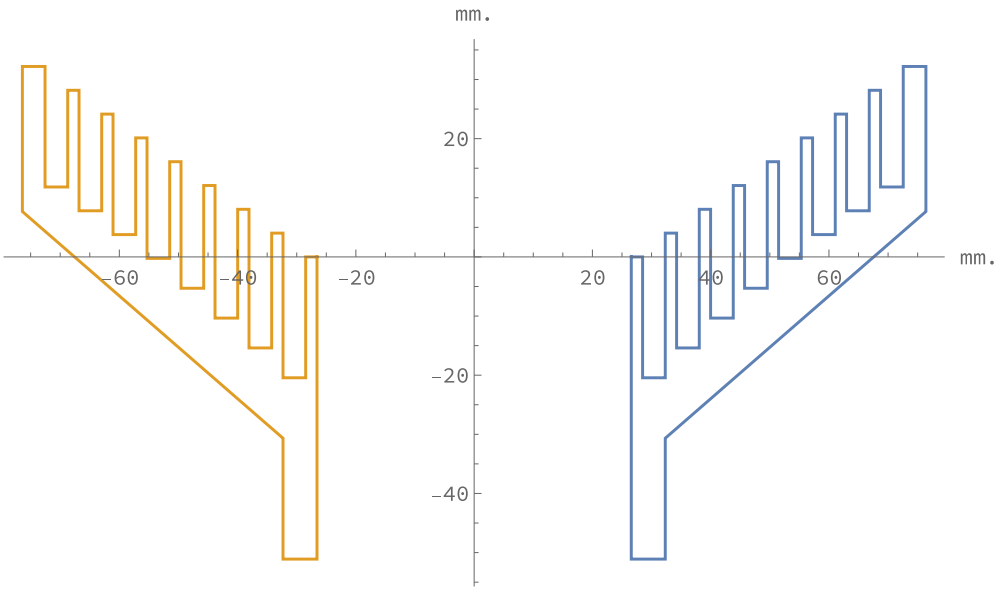

The feed pattern in Figure 13 has an edge taper slightly deeper than -16 db. However, when placed in the optics it has a slightly larger spillover than the perfect gaussian feed. This may be due to a difference in overall shape and possibly small phase errors in outer edges of the feed illumination. Otherwise, the pattern is almost perfectly rotationally symmetric and has small cross polarization which is zero in the principle planes and peaks in the diagonal planes.

Figure 13

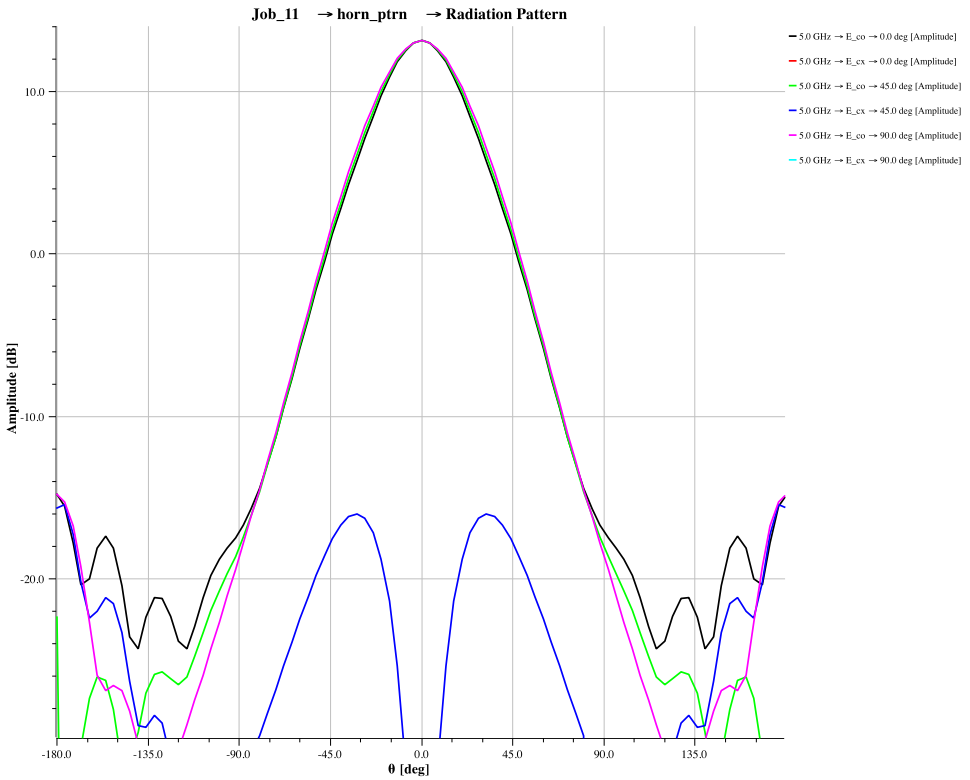

The illumination in the z=0 aperture plane is very similar to before. The diffraction ripple is a little more evident which may be due to this plot being generated with quadruple the number of data points. The deep cutoff at the edge is still the same. The interference effect on the left side is a little more extensive, evidence that the spillover from this horn feed is slightly larger than the perfect feed.

Figure 14

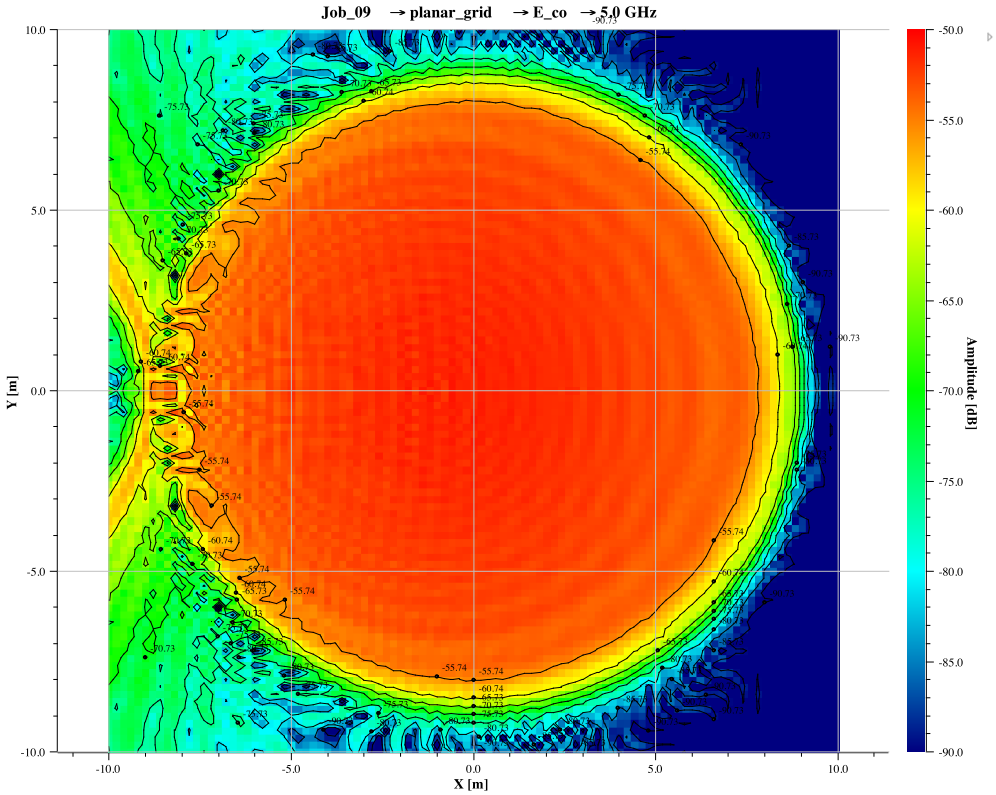

The close in beam pattern is shown is Figure 15. The peak gain is 58.9 dbi. which is slightly lower and corresponds to an overall efficiency of .87. The small drop in efficiency is partly caused by small phase errors in the real feed. Any realistic feed will have some phase errors in the low level parts of the pattern. Another difference is the increased cross polar level in the diagonal plane. Corrugated horns have a “four leaf clover” cross polar pattern and this is what causes the increased cross polar level. It is still quite small at about -32 db. below peak and the peak is outside the -3 db. level on the main beam. There is also a tiny asymmetry in the sidelobes.

Figure 15

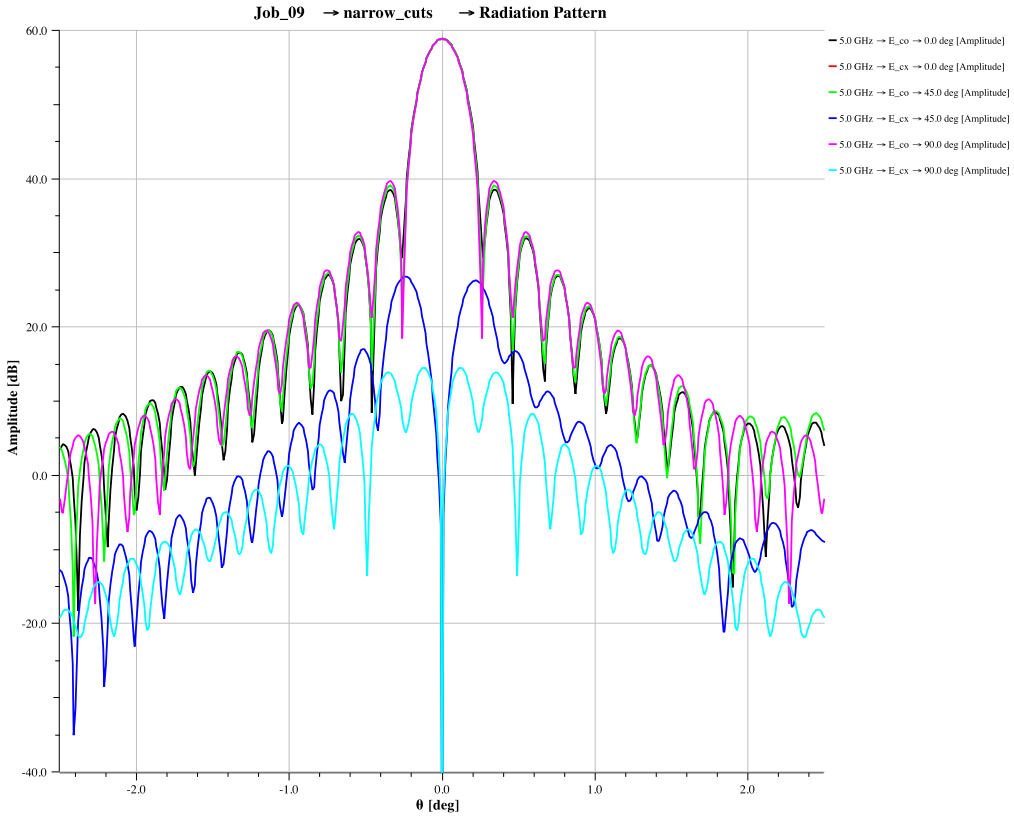

Figures 16, 17 show the pattern on the far field sphere. The slightly larger spillover of the feed past the secondary is evident. This will have a small effect on the tipping curve, especially feed down. Otherwise, all of the previous commentary holds.

Figure 16

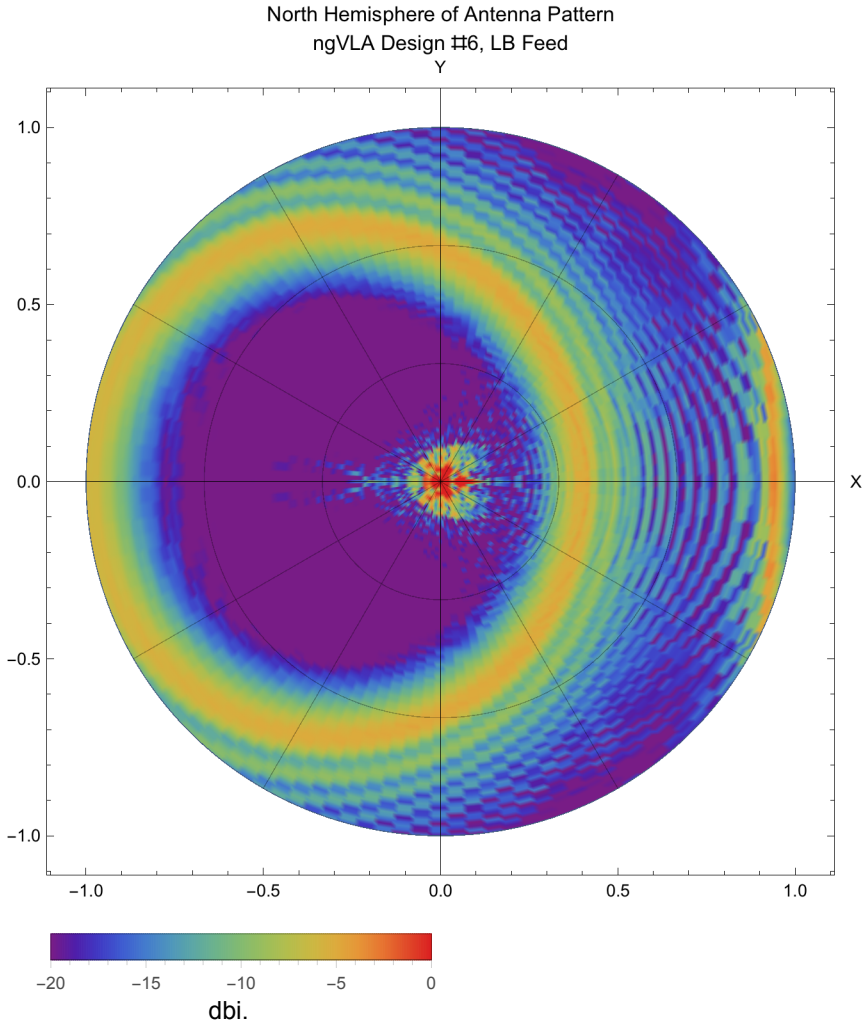
North Hemisphere of Antenna Pattern
ngVLA Design #6, LB Feed
Y
X
1.0
0.5
0.0
−0.5
−1.0
−1.0
−0.5
0.0
0.5
1.0
−20
−15
−10
−5
0
dbi.

Figure 17

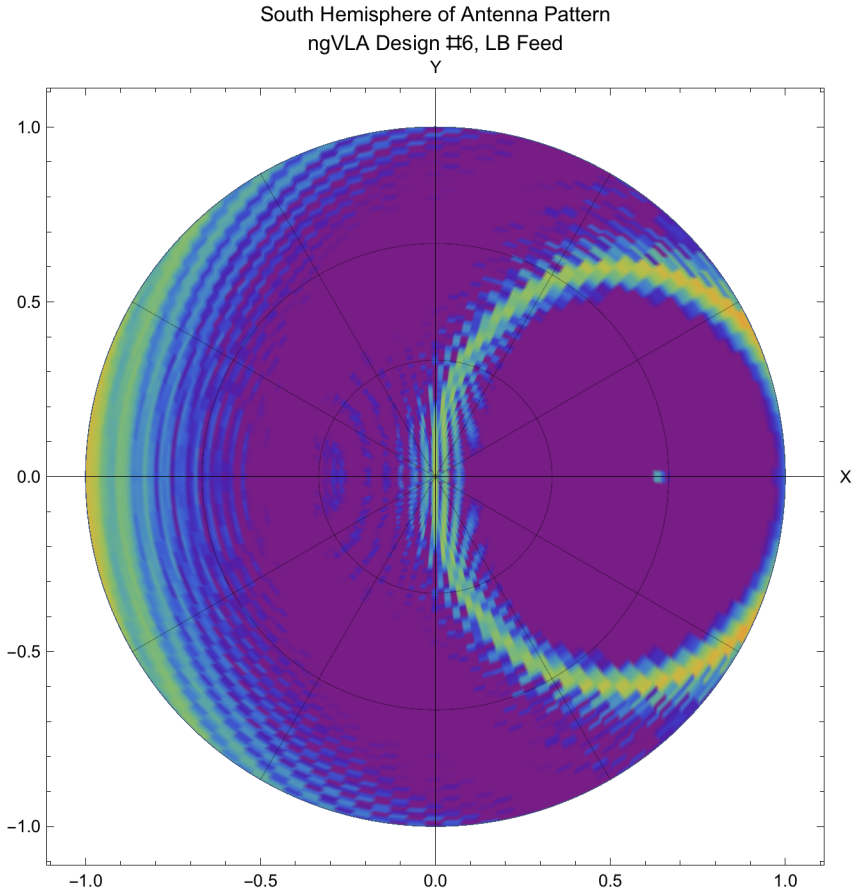

Figure 18 shows the wide angle far field pattern. All of the general features are the same with the peaks of the feed spillover being approximately 1 db. larger.

Figure 18

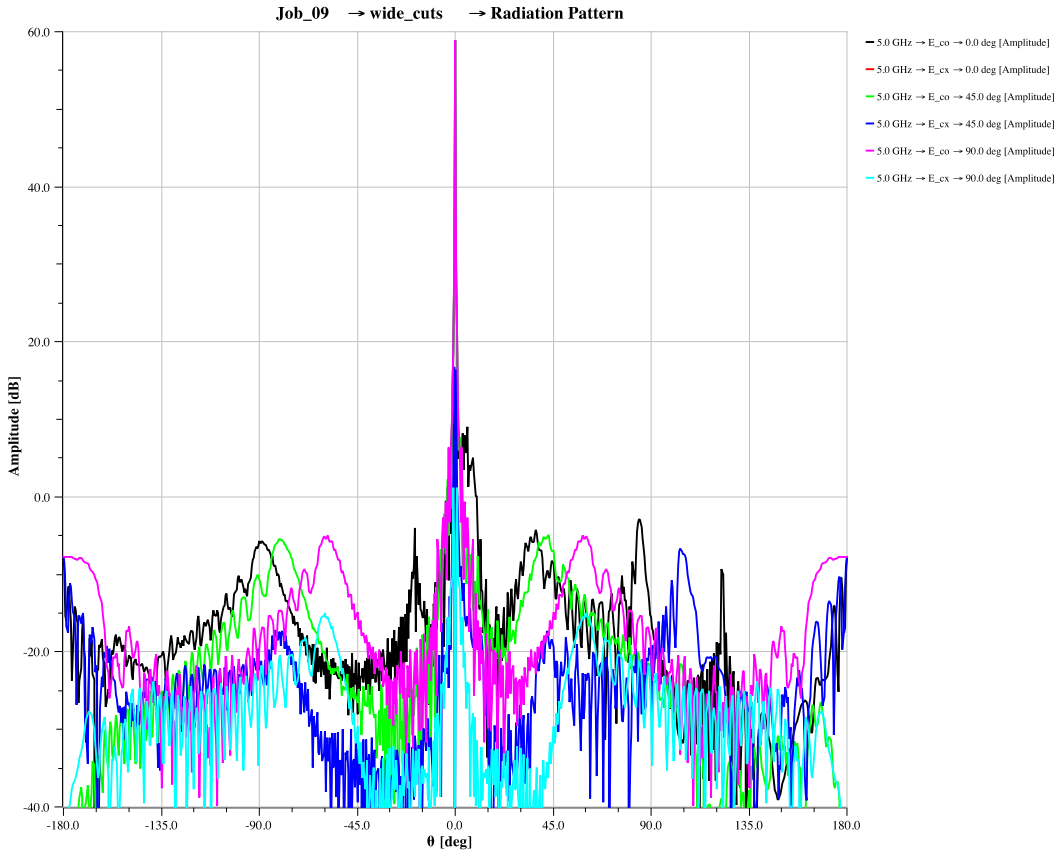

Tipping Curve with an Actual Feed

Figure 19 shows the tipping curve which is mostly similar to before with an extra .5 Kelvin at zenith and the feed down curve being somewhat worse. Again, for feed down a subreflector extension would likely improve the performance.

Figure 19

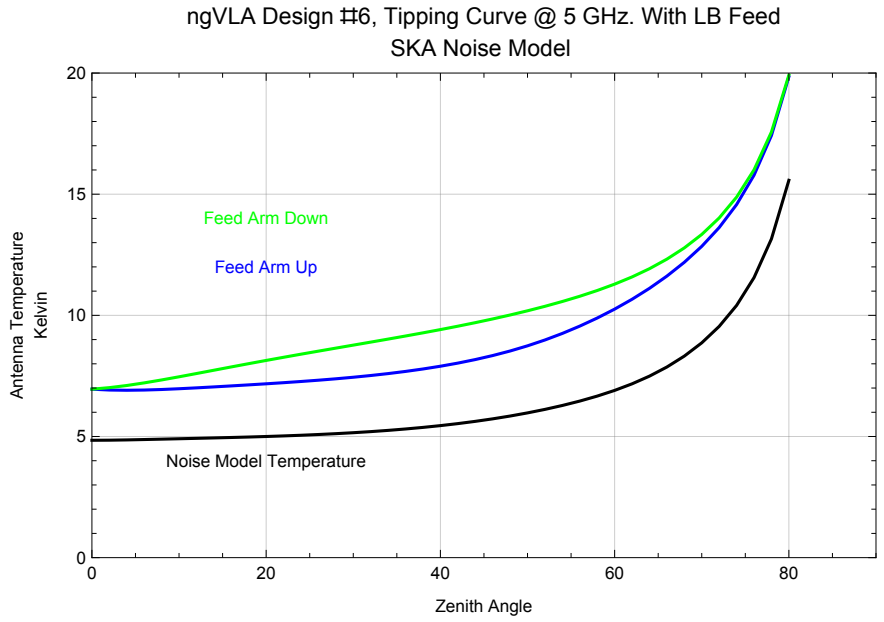

Figure 20

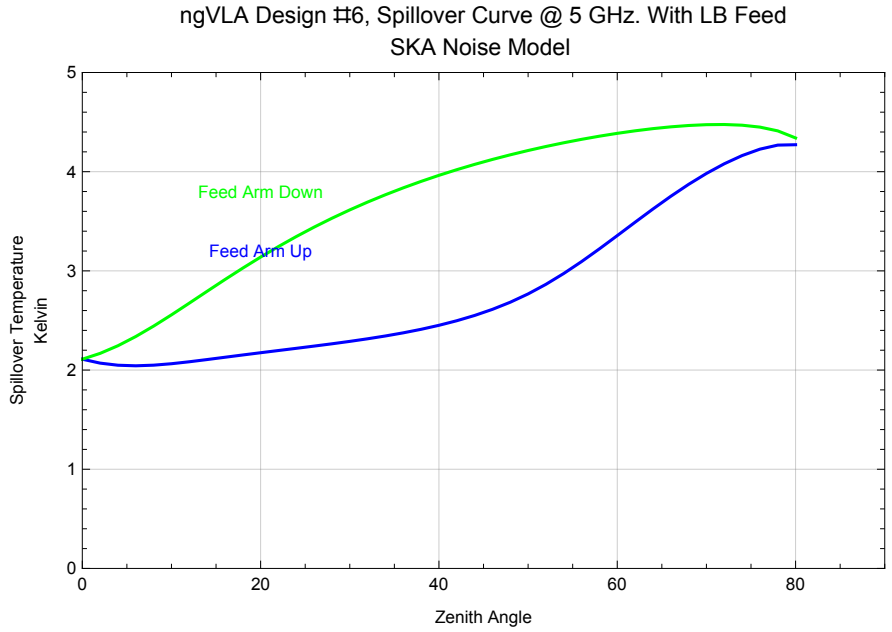

Conclusions

This first design for the ngVLA is very successful, achieving both high efficiency and very low antenna temperature. The performance with a realistic feed horn is very close to the performance with a mathematically perfect feed. It should be emphasized that the performance is dominated by the choice of feed. Other possible feeds should be analyzed in the optics to compare performance results. This first design could be modified with an extension on the subreflector or a modification to the optics to improve the feed down tipping. Review of the overall geometry from a structural perspective might suggest changes.